Journal of Power Sources 270 (2014) 379–385

Contents lists available at ScienceDirect

Journal of Power Sources

journal homepage: www.elsevier.com/locate/jpowsour

On the development of activated carbons with high affinity for high voltage propylene carbonate based electrolytes

C. Ramirez-Castro [a], C. Schütter [a], S. Passerini [a, b], A. Balducci [a, *]

[a] University of Muenster, MEET Battery Research Centre and Institute of Physical Chemistry, Corrensstr. 28/30, 48149 Münster, Germany
[b] Helmholtz Institute Ulm, Karlsruhe Institute of Technology, Albert Einstein Allee 11, Ulm, Germany

HIGHLIGHTS

- Activated carbon tailored for use in high voltage PC-based electrolytes.
- P4 is a microporous activated carbon.
- EDLCs containing P4 display high energy and power.

ARTICLE INFO

Article history:
Received 9 April 2014
Received in revised form
4 July 2014
Accepted 5 July 2014
Available online 24 July 2014

Keywords:
EDLCs
Activated carbon
High voltage PC-based electrolytes
Volumetric capacitance

ABSTRACT

In this work we report about the morphological and structural characteristic of an activated carbon (P4) tailored for use in high voltage PC-based electrolytes. In these types of electrolytes P4 displays specific capacitance of about 120 F g^{-1} and volumetric capacitance of 61.6 F cm^{-3}, which are very promising values in view of the realization of high energy EDLCs. We show that using P4 in combination with the electrolyte 1.5 M $PYR_{14}BF_4$ in PC it is possible to realize EDLCs able to deliver, at 1 A g^{-1}, specific energy and power of 34.5 Wh kg^{-1} and 1.7 kW kg^{-1}, respectively. These values are among the highest so far reported for this type of EDLCs. Furthermore, it also displays capacitance retention higher than 85% after 50.000 cycles. Taking into account these results, P4 appears therefore a suitable candidate for the realization of high energy EDLCs.

1. Introduction

Electrochemical double layer capacitors (EDLCs), also known as supercapacitors, are today advancing as one of the most promising energy storage technology. EDLCs feature high power (up to 10 kW kg^{-1}) and an extremely high cycle life (>500,000) and they are currently used in a large number of applications where rapid charge–discharge capability and reliability are required [1]. The commercially available EDLCs contain activated carbon (AC) as active materials and electrolytes containing either propylene carbonate (PC) or acetonitrile (ACN) as solvent and tetraethyl ammonium tetrafluoroborate (Et_4NBF_4) as conductive salt [2,3]. The operative voltage of these EDLCs is in the range of 2.3–2.7 V [4].

An increase of the EDLCs energy would allow the introduction of these high power devices in a larger number of applications and, consequently, it would increase the market size of EDLCs. Therefore, in the last years many efforts have been made to increase the energy of EDLCs.

The most effective strategy to increase the energy and the power of EDLCs is to increase their operative voltage [4]. In EDLCs the charge is electrostatically stored at the electrode–electrolyte interface and the operative voltage of these devices is dependent on the electrochemical stability of the electrolyte. Several studies showed that it is not possible to increase the operative voltage of EDLCs using the state-of-the-art electrolytes without negative effect on their cycling stability [5,6]. Therefore, in the last years many efforts have been directed on the development of alternative electrolytes for high voltage EDLCs. Different ionic liquids (ILs) and alternative organic solvents have been investigated and promising results have been obtained [3,7–12].

Recently, we proposed the use of innovative PC-based electrolytes, containing different conducting salts with respect to the conventional PC-based electrolytes, for the realization of high voltage, high energy EDLCs [13]. These innovative electrolytes exhibit high conductivity, low viscosity and large electrochemical stability. Additionally, they have the advantage of being highly

* Corresponding author.
E-mail address: andrea.balducci@uni-muenster.de (A. Balducci).

http://dx.doi.org/10.1016/j.jpowsour.2014.07.035
0378-7753/

concentrated, which is a key aspect in view of the realization of high energy EDLCs. We showed that the use of these innovative electrolytes allows the realization of EDLCs which are able to display higher energy and power, compared to the state-of-the-art electrolytes, in a broad range of current densities. For that, they can certainly be considered as promising electrolytes for the realization of advanced EDLCs.

As mentioned above, in EDLCs the charge is electrostatically stored at the electrode–electrolyte interface. Therefore, it is clear that in order to develop high energy EDLCs not only the electrolyte, but also the electrode materials need to be considered. Particularly, the affinity between the electrode materials and the electrolyte should be carefully considered. Parameters like the specific surface area, the pore size distribution and the chemical environment in the carbon-electrode material as well as the effective ion size and wettability in the electrolyte have to be taken into consideration in order to ensure an optimal operation of the final device [1,5].

In the last years, due to their interesting properties several carbonaceous materials, e.g. carbon blacks, carbon aerogels or carbon nanotubes have been proposed as alternatives for ACs [4,14]. Nevertheless, up to now the most suitable material for the realization of high energy EDLCs is AC due to its high surface area and low cost. ACs are obtained from carbon-rich organic precursors by carbonization in inert atmosphere followed by a physical or chemical activation. While in the last years, several studies have focused on the development of ACs in order to optimize their performance in either aqueous or organic conventional electrolytes, a lower number of works dealt with tailoring ACs for innovative electrolytes, e.g. ionic liquids and high voltage PC-based electrolytes. [9,15,16].

In this manuscript we report about an activated carbon (P4) tailored for being used in high voltage PC-based electrolytes. Initially, the morphology, specific surface area, pore size distribution and oxygen content of this innovative AC are considered and compared with those of a commercial available AC. Afterward, the use of both ACs in EDLCs containing high voltage PC-based electrolytes is investigated with the aim to understand the benefit related to the use of this tailored activated carbon on the energy of high voltage EDLCs.

2. Experimental

2.1. Materials

The activated carbon P4 supplied by SGL group was used as received. For comparison, all the physicochemical characterization and the electrochemical tests were also realized for Norit DLC super 30 (Norit).

The carbonaceous materials were tested in three different electrolytes; 1 M Et_4NBF_4 in PC, 1.5 M *N*-methyl-*N*-butyl pyrrolidinium bis-[(trifluoromethyl)sulfonyl]imide ($PYR_{14}TFSI$) in PC and 1.5 M *N*-methyl-*N*-butyl pyrrolidinium tetrafluoroborate ($PYR_{14}BF_4$) in PC. The organic salt Et_4NBF_4 (Sigma–Aldrich) and the ionic liquid $PYR_{14}TFSI$ (Iolitec, Germany) were dried under vacuum and stored in a glove box while the $PYR_{14}BF_4$ was synthesized as described in Ref. [17]. The propylene carbonate (Sigma–Aldrich) was used as received.

2.2. Physicochemical characterization

The morphologies of the carbon powders were investigated by Scanning Electron Microscopy (SEM) AURIGA FIB-SEM from ZEISS. The samples were dispersed in ethanol by ultrasound and two or three drops of the dispersed powder were deposited on the sample holder and dried in an oven at 60 °C before analysis.

The elemental composition of the carbons was determined by CHN- and XPS analysis. For CHN analysis a CHNO-Rapid (Heraeus) was used. By combusting a small amount of carbon in excess oxygen atmosphere and qualitative analysis of the combustion product, the composition of the sample can be calculated.

An AXIS ULTRA HSA Kratos was utilized using the Al Kα monochromatic beam (1486.7 eV). Core level spectra (pass energy of 20 meV) were used to evaluate the atomic concentration of the species present at the surface of the samples. The sample powders were dispersed onto adherent carbon film. The data were collected at room temperature and typically the operating pressure in the analysis chamber was kept below 10^{-9} Torr. Data analyses were performed with the Casa XPS-Kratos, where every spectrum was corrected according to C 1s at 284.5 eV (graphite like carbon).

Raman measurements were made on a Bruker SENTERRA dispersive Raman microscope (20X magnification) with a green semiconductor-laser (532 nm, 20 mW). The dispersive element was a grating with 400 lines/mm and the aperture was a slit with the dimensions of 50 × 1000 microns. The powder samples were mounted on glass slides.

In order to gain information of the porous structure of the carbon, adsorption of nitrogen at 77 K was performed on an ASAP 2020 Surface Area and Porosity Analyzer (*Micromeritics*). All samples were degassed at 350 °C for 6 h under vacuum before the adsorption experiment was started. The specific surface area (SSA) of the carbons was determined from N_2 adsorption isotherm using the BET equation and the DFT model (cumulative DFT surface area). The total micropore volume (V_{micro}) and the average pore diameter (L_0) were calculated by applying the Dubinin–Radushkevich (DR) equation to the N_2 isotherm by assuming slit-shaped pores [18]. The total pore volume (TPV) was obtained from the N_2 adsorption at $P/P_0 = 0.99$ and the volume of the mesopores (V_{meso}) was estimated by subtracting the total micropore volume from the total pore volume.

2.3. Electrochemical characterization

The electrodes were prepared following a procedure reported in Ref. [19]. The weight ratio between the active material (P4/Norit), the conductive additive (Super C65, Timcal) and the binder (Sodium carboxymethyl-cellulose, CMC 2000, Walocell) was 90:5:5 with a mass loading of 5–6 mg cm^{-2} and an area of 1.13 cm^2. The final electrode density (coating) was 0.50 g cm^{-3} for Norit and 0.57 g cm^{-3} for P4.

Electrochemical test were carried out in a two electrodes configuration Swagelock® type cell. The cells were assembled in an Argon-filled glove box with oxygen and water contents lower than 1 ppm. For the working and the counter electrode, two identical activated carbon electrodes were used (symmetric EDLCs). As separator, a Whatman GF/D glass microfiber filter soaked with 100 μL of the corresponding electrolyte was used.

The electrochemical tests were performed at 20 °C a VMP multichannel potentiostatic–galvanostatic system (Biologic Science Instrument, France). Cyclic voltammetry were performed at 20 mV s^{-1} while galvanostatic charge–discharge tests were carried out using current densities ranging from 1 to 10 A g^{-1}. The charge/discharge long term cycling tests were carried out over 50,000 cycles at 1 A g^{-1}. The values of capacitance of the total active material in the cell (C), the equivalent series resistance (ESR), the coulombic efficiency (η), average energy (E) and average power (P) have been calculated as indicated in Refs. [20,21].

3. Results and discussions

Fig. 1 show the SEM images of P4 and Norit at two different magnifications. According to Fig. 1a and b, both carbons exhibit

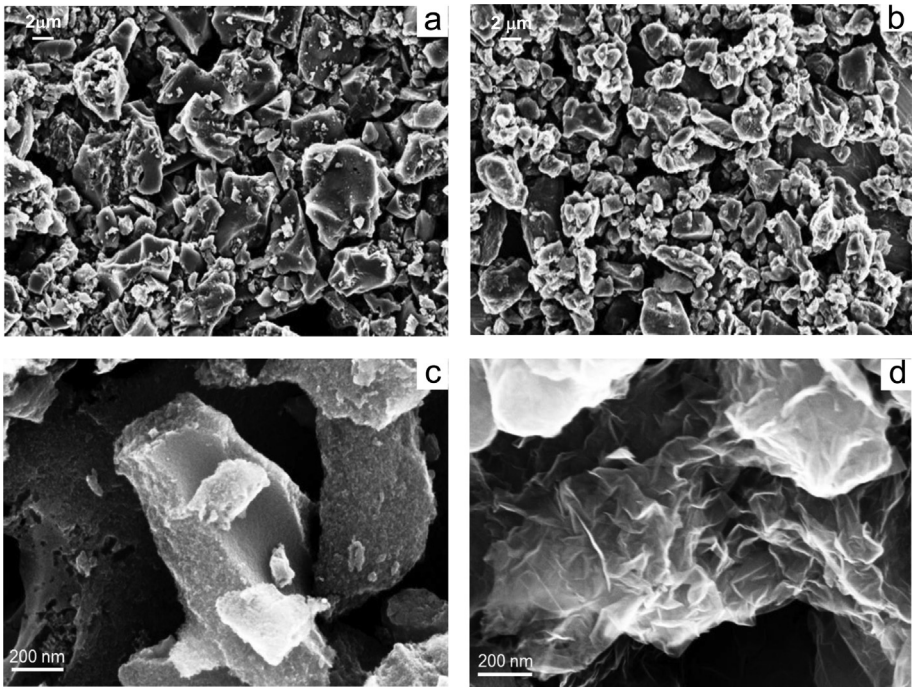

Fig. 1. SEM images of carbon Norit (a and c) and P4 carbon (b and d).

irregular shapes and sizes in the order of micrometers to nanometers. At higher magnifications, Norit (c) displays a regular and flat surface while P4 surface (d) comprises a thin and wrinkled sheets-like structure.

Elemental analysis of P4 and Norit revealed a carbon content of 96.1% and 94.4%, respectively (Table 1). Both materials present an oxygen content of around 5%. By XPS, the atomic percentage of C and O are in agreement with the CHN analysis. These results evidence the homogeneity in the chemical environment of the bulk and the surface in both carbons.

Fig. 2 compares the Raman spectra of the two investigated carbons. For both materials two main spectral peaks are observed around 1340 and 1590 cm^{-1} which correspond to the D and G band respectively, where the D band is related to the disorder domains in the carbon structure and the G band to the graphite domains [22]. The intensity ratio of D band to G band (I_D/I_G) in P4 carbon is lower with respect to Norit and is related to a more crystalline structure. Since the preferential sites for the formation of oxygen functionalities are on the defects or edges of carbonaceous materials [23], the results found by Raman analysis are in agreement with XPS analysis where a lower oxygen content for P4 is detected. In the case of P4 carbon, the spectral peak at 1590 cm^{-1} exhibits a slight shoulder after 1600 cm^{-1}, this shoulder arises from the graphite edge-plane [24] also observed by SEM.

Table 2 and Fig. 3 report the data obtained from the adsorption isotherms and porosity measurements. As shown in Fig. 2a, the N_2 adsorption isotherms for both carbons are of type I, corresponding to microporous materials [25]. Amongst the two carbons, Norit appears to possess the highest adsorption capacity; which is translated in a larger surface area with respect to P4. Since it is well documented that the determination of the surface by the BET model leads to an overestimation of the surface of microporous activated carbons [26], the DFT model was also used to evaluate the specific surface area of P4 and Norit (see Table 2). In terms of porosity (Fig. 3b), P4 has most of its pores in the microporosity range (up to 2 nm) with a L_0 centered at 1.87 nm, while Norit has a significant amount of mesopores (around 9%) with a L_0 centered at 2.51 nm. Y. Yang [27] suggested that in carbonaceous materials with sheets-like structures as P4, the mesopores are derived from the incompact stacking, entanglement and overlap of the sheets, while the micropores probably come from defects in the sheets.

Considering the results reported above, P4 and Norit appear to display significant differences in term of surface area, average pore width and pore size distribution. Norit displays a higher surface

Table 1
Elemental analysis and XPS data for P4 and Norit.

Sample	C_{CHN} (%)	H_{CHN} (%)	$O_{CHN\text{-}diff}$ (%)	C_{xPS} (%)	O_{xPS} (%)
P4	96.1	0.3	3.6	96.2	3.8
Norit	94.4	0.4	5.2	94.9	5.1

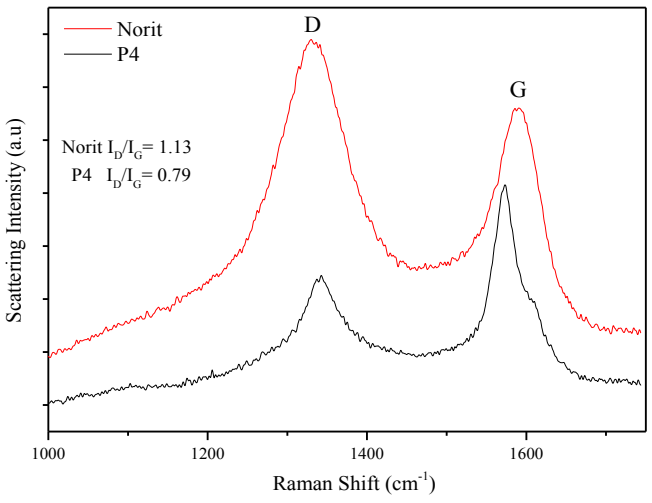

Fig. 2. Comparison of the Raman spectra of Norit and P4.

Table 2
Textural characterization of P4 and Norit.

Sample	BET-area ($m^2\ g^{-1}$)	DFT-area ($m^2\ g^{-1}$)	TPV ($cm^3\ g^{-1}$)	V_{micro} ($cm^3\ g^{-1}$)	V_{meso} ($cm^3\ g^{-1}$)	V_{micro}/V_{meso} ($cm^3\ g^{-1}$)	L_0 (nm)
P4	1104	957	0.605	0.601	0.004	150.25	1.870
Norit	1500	1138	0.850	0.780	0.070	11.14	2.510

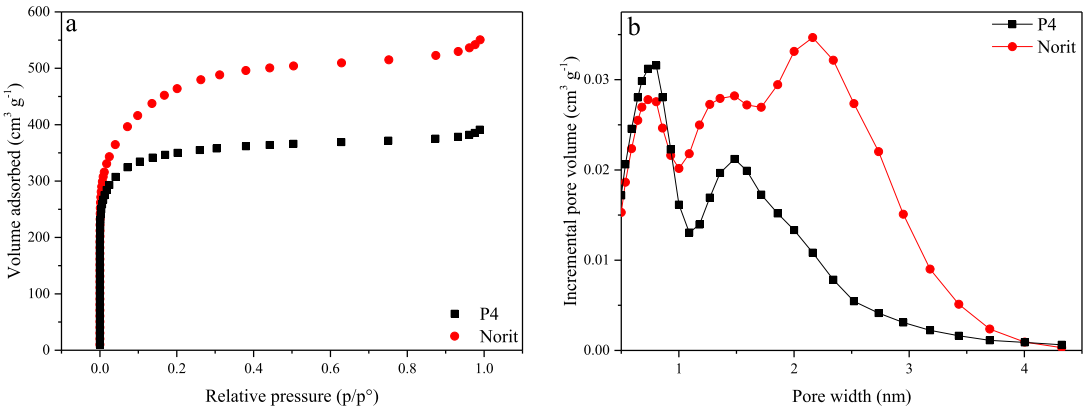

Fig. 3. a) N_2 adsorption isotherms at 77 K and b) pore size distribution of Norit and P4.

area compared to P4. On the other hand, the average pore width of P4 is significantly smaller compared to the one of Norit. Furthermore, it is interesting to notice the different amount of mesopores present on these two carbons. As shown in Fig. 3 and indicated in Table 2, P4 displays a very low amount of mesopores compared to Norit. Consequently, the ratio between micro and mesopores is completely different in P4 and Norit and P4 can be seen as a much more "microporous" carbon compared to Norit.

Fig. 4 compares the voltammetric profiles of electrodes containing the activated carbons P4 and Norit in the conventional electrolytes 1 M Et_4NBF_4 in PC (3-electrode configuration cell). As show, the P4 electrode displays a specific capacitance of 120 F g^{-1}. This value is significantly higher than that of the Norit electrode, which displays a specific capacitance in the order of 95 F g^{-1}. It is also very interesting to remark that the volumetric capacitance of P4 (61.6 F cm^{-3}) is significantly higher than that of Norit (42.8 F cm^{-3}). Since the DFT surface area of Norit is higher than P4, the higher capacitance displayed by P4 seem to indicate that this

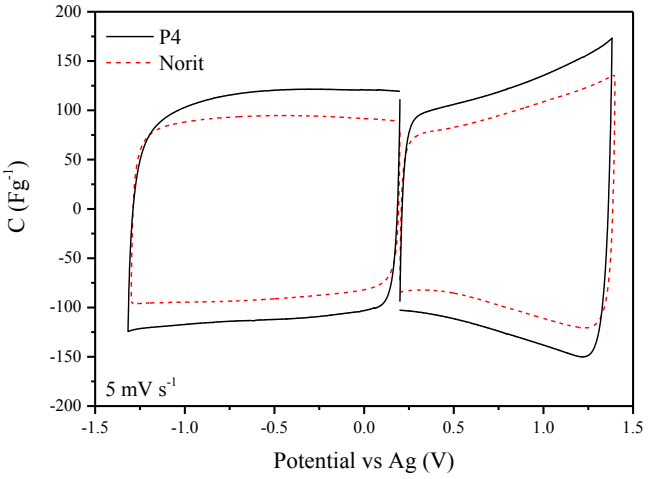

Fig. 4. Comparison of the voltammetric profiles of the electrodes containing P4 and Norit as active materials in 1 M Et_4NBF_4 in PC (scan rate 5 mV s^{-1}).

carbon possesses a higher effective surface area compared to Norit, which can be related to its structure and surface characteristics. As mentioned by Chmiola et al. [28], the presence of a high number of micropores is beneficial for an optimal utilization of the electrolyte ions due to a stronger interaction between the ions and the pore walls. Furthermore, it is also interesting to notice that the ion size of electrolytes, which is comprise between 0.7 and 1.1 nm, appears to match very well with the pore width of P4 (1.8 nm) [9]. Using the activated carbons P4 and Norit as active materials, EDLCs and tested in the electrolytes 1 M Et_4NBF_4 in PC, 1.5 M $PYR_{14}TFSI$ in PC and 1.5 M $PYR_{14}BF_4$ in PC. Fig. 5 compares the voltammetric profiles of the devices as obtained during test carried out at room temperature using a scan rate of 20 mV s^{-1}. As shown, all EDLCs display the typical rectangular shape characteristic of a pure capacitive behavior [29]. Nevertheless, is important to highlight that in all electrolytes the EDLCs containing P4 exhibit values of capacitance at least 5 F g^{-1} higher than the ones containing Norit, as expected because of the higher capacitance of this carbon compared to the one of Norit. For P4 in the electrolytes 1.5 M $PYR_{14}TFSI$ in PC and 1.5 M $PYR_{14}BF_4$ in PC a tenuous wave near to 2.7 V on the positive side of the CV as well as a slight deviation of the ideal capacitive behavior when the potential scan is reversed in the positive-charge electrode region are observed in the EDLCs (Fig. 5b and c, respectively). Since the oxygen content of the two carbons is similar, but Norit is exempt of this behavior, a possible explanation for this deviation from the ideal rectangular shape could be the occurrence of some minor ion sieving process in P4. The occurrence of such process could be further investigated. Nevertheless, considering the very limited entity of such a process, it is reasonable to suppose that such process should not significantly affect the behavior of the EDLCs.

The results shown above indicate P4 as a promising activated carbon for EDLCs. To the best of our knowledge, the capacitance (both gravimetric and volumetric) exhibit by the activated carbon P4 is among the highest so far reported for this type of carbon in non-conventional electrolyte for EDLCs [8,9,17]. Thus, P4 appears as a promising candidate for the realization of high energy EDLCs.

In order to further investigate the performance of EDLCs containing P4 as active material, galvanostatic charge–discharge tests have been carried out using all three electrolytes. For the tests,

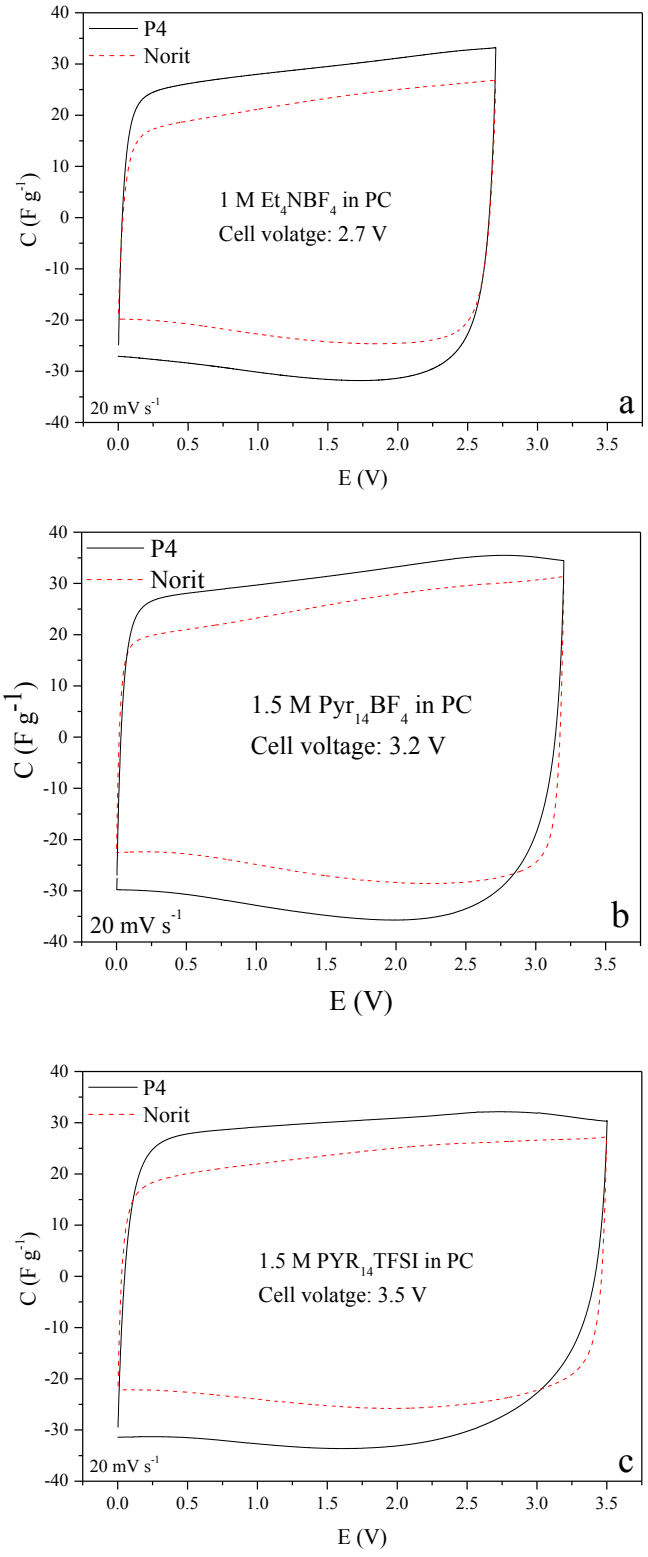

Fig. 5. Cyclic voltammetry (scan rate 20 mV s^{-1}) of EDLCs containing P4 and Norit carbon as active material in a) 1 M Et_4NBF_4 in PC, b) 1.5 M $PYR_{14}BF_4$ in PC c) at 1.5 M $PYR_{14}TFSI$ in PC.

currents ranging from 1 A g^{-1} to 10 A g^{-1} were used. The operative voltage used for this investigation was 2.7, 3.2 and 3.5 V for 1 M Et_4NBF_4 in PC, 1.5 M $PYR_{14}BF_4$ in PC and 1.5 M $PYR_{14}TFSI$ in PC [17,30], respectively. In all electrolytes the coulombic efficiency of the charge–discharge was close to 100% through all cycling and applied currents. The equivalent series resistance of the EDLCs was in the order of 6–7 Ω cm^2 for the EDLCs containing both P4 and Norit as active material. As shown in Fig. 6, when a current density of 1 A g^{-1} was applied, the EDCLs containing P4 displayed a specific capacitance in the order of 30 F g^{-1} (referred to the total active material) in all three electrolytes. On the other hand, the EDLCs containing Norit displayed a specific capacitance in the order of 23–25 F g^{-1}, which is a value of about 20% lower compared to the P4. When higher current densities were applied, the capacitance of the EDLCs decreased, but with different magnitude for each electrolyte. Here the capacitance-rate dependence was better for 1 M Et_4NBF_4 in PC, followed by 1.5 M $PYR_{14}BF_4$ in PC and finally 1.5 M $PYR_{14}TFSI$ in PC. This trend is obviously related to the viscosity and conductivity of the three electrolytes and it is in agreement with the results already reported in literature [13]. It is important to notice that the used active materials had an effect on the capacitance-rate dependence and, in all electrolytes, the EDLC containing Norit displayed better rate dependence than the one containing P4. This different behavior is most likely related to the morphology and pore size distribution of the two investigated activated carbons. As shown above, while most of the pore volume in P4 is composed of micropores, Norit presents a considerable amount of mesopores. These mesopores are the pathways, which lead to quick ion-transport into the micropores, and, as a consequence, are necessary when high regimes are required in EDLCs applications [31,32]. Therefore, the poorest capacitance-rate

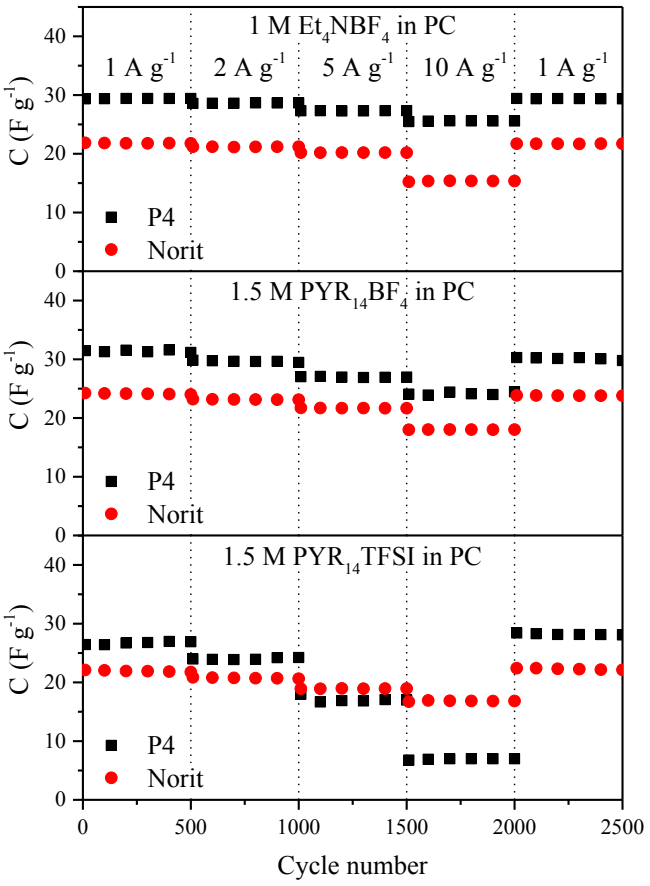

Fig. 6. Evolution of specific capacitance at different currents of EDLCs containing P4 and Norit carbon as active material in the electrolytes 1 M Et_4NBF_4 in PC, 1.5 M $PYR_{14}BF_4$ in PC and 1.5 M $PYR_{14}TFSI$ in PC. The operative voltages for this test were 2.7 V, 3.2 V and 3.5 V, respectively.

dependence behavior observed for P4 can be associated to its low amount of mesopores.

Fig. 7, displays the average energy and power of the investigated devices. The mass used for the calculation refers to the sum of the active mass of both positive and negative electrodes. As shown, P4 exhibits promising results in terms of energy and power for the different electrolytes compared to Norit, as EDLCs based on this material are able to deliver higher specific power and energy for the organic electrolyte and the $PYR_{14}BF_4$ based electrolyte. In fact, the combination of P4 and 1.5 M $PYR_{14}BF_4$ in PC yields the highest energy and power values for all current densities, for example at 1 A g^{-1} such an EDLC delivers a specific energy and power of 34.5 Wh kg^{-1} and 1.7 kW kg^{-1}, respectively, which is an increase of 43% in terms of energy and 16% in terms of power compared to Norit. At higher currents, however, this margin decreases to 15% energy gain and 4% power gain for P4, indicating that Norit is handling the high currents better than P4 for this electrolyte. The reason for this decrease in performance at higher rates is most likely due to the absence of mesopores in P4 compared to Norit, as mentioned before. This could also explain why the EDLC based on P4 and 1.5 M $PYR_{14}TFSI$ in PC has the worst performance of all despite using an operative voltage of 3.5 V: without mesopores the big ions of $PYR_{14}TFSI$ can barely access the micropores, limiting the performance of the device at higher rates. Since the other electrolyte using the PYR_{14}-cation does not suffer as much at higher rates, the limiting factor is presumably the TFSI-anion. If we consider a scale factor of 4 for the transfer of lab scale devices to real devises [33], the average energy and power density of the EDLC based on P4 and 1.5 M $PYR_{14}BF_4$ in PC can be estimated in the order of 8.6 Wh kg^{-1} and 0.4 kW kg^{-1}, respectively. It is interesting to note that, although the power density is lower for our device, the value for the energy density is considerately higher than those of commercially available EDLCs based on PC or acetonitrile [34].

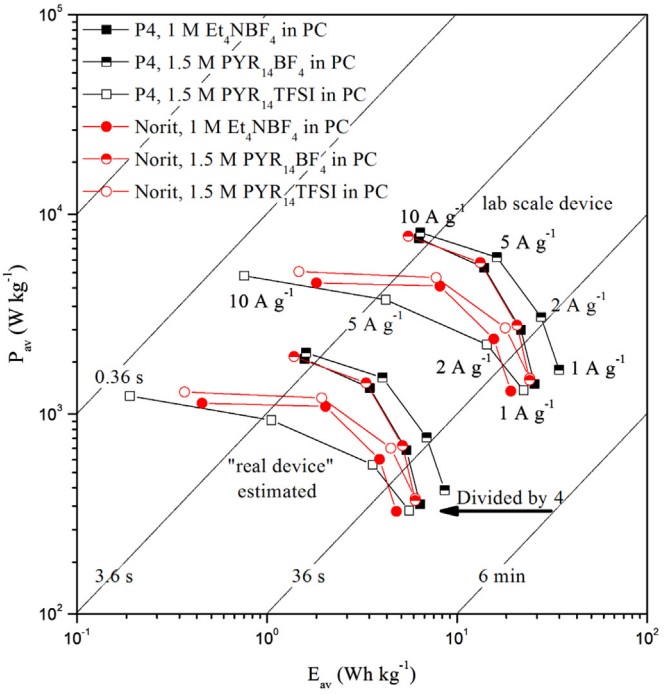

Fig. 7. Ragone plot of EDLCs containing P4 and Norit carbon as active material in the electrolytes 1 M Et_4NBF_4 in PC, 1.5 M $PYR_{14}BF_4$ in PC and 1.5 M $PYR_{14}TFSI$ in PC. Both average energy and power are referred to the total mass of active materials of both electrodes.

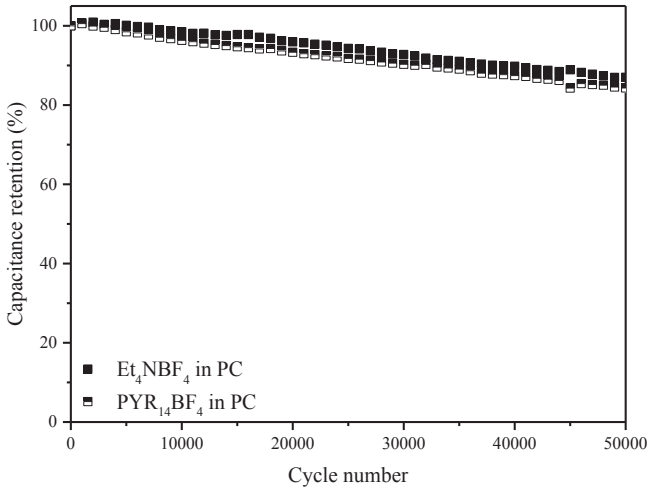

Fig. 8. Cycling stability of EDLCs containing P4 carbon as active material in the electrolytes 1 M Et_4NBF_4 in PC and 1.5 M $PYR_{14}BF_4$ in PC, using an operative voltage of 2.7 V and 3.2 V, respectively.

Finally due to the promising results of P4 in terms of energy and power, the cycling stability of this material was also investigated using 1 M Et_4NBF_4 in PC and 1.5 M $PYR_{14}BF_4$ in PC as electrolyte, with an operative voltage of 2.7 V and 3.2 V, respectively. The applied current density for this test was 1 A g^{-1}. As shown in Fig. 8, in both electrolytes the EDLCs follow the same trend during cycling, displaying capacitance retention values up to 85% over 50,000 cycles. To further investigate the stability of the P4-based EDLCs, also float test were carried out. The EDLCs based on P4 were kept at the maximum operative voltage (2.7 V for 1 M Et_4NBF_4 in PC and 3.2 V for and 1.5 M $PYR_{14}BF_4$ in PC) for 200 h at a temperature of 20 °C. As shown in Fig. 9, the EDLCs containing 1.5 M $PYR_{14}BF_4$ in displayed a very stable behavior during the test and decrease of specific capacitance of only 2.5% was observed after 200 h. In comparison, the PC/$PYR_{14}BF_4$ based device already looses about 12% of the initial capacitance after 200 h. This capacitance fading is in line with those already reported in literature [14] and it is most likely originated by the high applied voltage of 3.2 V.

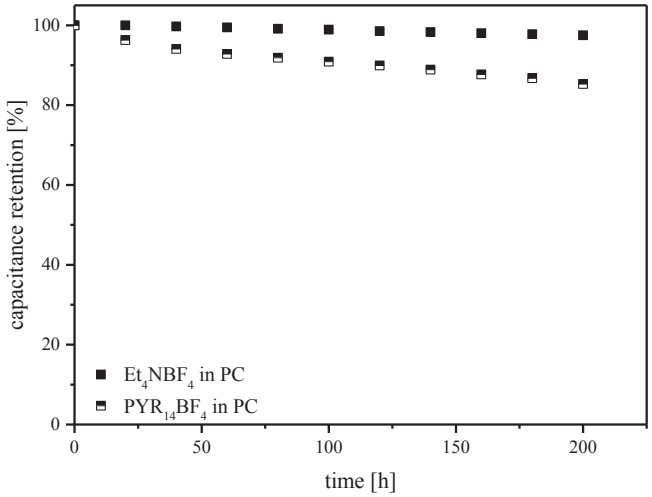

Fig. 9. Capacitance retention of EDLCs containing P4 as active material in the electrolytes 1 M Et_4NBF_4 in PC and 1.5 M $PYR_{14}BF_4$ in PC observed for 200 h float test carried out at 2.7 V and 3.2 V, respectively.

These results, together with the energy and power values acquired here, make of P4 carbon a good candidate for future applications where high voltage PC-based electrolytes are needed.

4. Conclusions

In this work we reported about the morphological and structural characteristic of an activated carbon (P4) tailored for use in high voltage PC-based electrolytes. P4 displays a rather marked "microporous" character and a relatively low amount of mesopores. We showed that this carbon displays in high voltage PC-based electrolytes a specific capacitance of about 120 F g^{-1}, which is a very promising values in view of the realization of high energy EDLCs. Using P4 in combination with the electrolyte 1.5 M $PYR_{14}BF_4$ in PC it is possible to realize EDLCs able to deliver, at 1 A g^{-1}, specific energy and power of 34.5 Wh kg^{-1} and 1.7 kW kg^{-1}, respectively. These values are among the highest so far reported for this type of EDLCs. The investigated EDLCs display promising performance also when higher current densities (up to 10 A g^{-1}) are applied. Furthermore, it also displays a capacitance retention higher than 85% after 50,000 cycles. Taking into account these results, P4 appears therefore a suitable candidate for the realization of high energy EDLCs.

Acknowledgments

The authors wish to thank the Bundesministerium für Bildung and Forschung (BMBF) for the financial support within the project IES (contract number 03EK3010).

References

[1] P. Simon, Y. Gogotsi, Nat. Mater. 7 (2008) 845–854.
[2] Philippe Azais, L. Duclaux, P. Florian, D. Massiot, M.-A. Lillo-Rodenas, A. Linares-Solano, J.-P. Peres, C. Jehoulet, F. Béguin, J. Power Sources 171 (2007) 1046–1053.
[3] F. Beguin, E. Frackowiak, Supercapacitors; Materials, Systems and Applications, Wiley-VCH, 2013.
[4] C. Arbizzani, M. Biso, D. Cericola, M. Lazzari, F. Soavi, M. Mastragostino, J. Power Sources 185 (2008) 1575–1579.
[5] R. Kötz, M. Hahn, P. Ruch, R. Gallay, Electrochem. Commun. 10 (2008) 359–362.
[6] M. Hahn, R. Kötz, R. Gallay, A. Siggel, Electrochim. Acta 52 (2006) 1709–1712.
[7] A. Brandt, P. Isken, A. Lex-Balducci, A. Balducci, J. Power Sources 204 (2012) 213–219.
[8] E. Perricone, M. Chamas, L. Cointeaux, J.-C. Lepretre, P. Judeinstein, P. Azais, F. Beguin, F. Alloin, Electrochim. Acta 93 (2013) 1–7.
[9] S. Pohlman, B. Lobato, T. Centeno, A. Balducci, Phys. Chem. Chem. Phys. 15 (2013) 17287–17294.
[10] R. Lin, P.-L. Taberna, S. Fantini, V. Presser, C.R. Pérez, F. Malbosc, N. Rupesinghe, K. Teo, Y. Gogotsi, P. Simon, J. Phys. Chem. Lett. 2 (2011) 2396–2401.
[11] R. Lin, P. Huang, J. Ségalini, C. Largeot, P.L. Taberna, J. Chmoila, Y. Gogotsi, P. Simon, Electrochim. Acta 54 (2009) 7025–7032.
[12] F. Soavi, C. Arbizzani, M. Mastragostino, J. Appl. Electrochem. 44 (2014) 491–496.
[13] A. Brandt, A. Balducci, J. Power Sources 250 (2014) 343–351.
[14] A.G. Pandolfo, A.F. Hollenkamp, J. Power Sources 157 (2006) 11–27.
[15] W.-Y. Tsai, R. Lin, S. Murali, L. Zhang, J. McDonough, R. Ruoff, P.-L. Taberna, Y. Gogotsi, P. Simon, Nano Energy 2 (2013) 403–411.
[16] R. Mysyk, V. Ruiz, E. Raimundo-Pinero, R. Santamaria, F. Béguin, Fuel Cells 10 (2010) 834–839.
[17] S. Pohlmann, A. Balducci, Electrochim. Acta 110 (2013) 221–227.
[18] A. Brandt, A. Balducci, J. Electrochem. Soc. 159 (2012) A2053–A2059.
[19] R.-S. Kühnel, N. Böckenfeld, S. Passerini, M. Winter, A. Balducci, Electrochim. Acta 56 (2011) 4092–4099.
[20] A. Balducci, R. Dugas, P.L. Taberna, P. Simon, D. Plée, M. Mastragostino, S. Passerini, J. Power Sources 165 (2007) 922–927.
[21] A. Krause, P. Kossyrev, M. Oljaca, S. Passerini, M. Winter, A. Balducci, J. Power Sources 196 (2011) 8836–8842.
[22] Z. Xu, M. Yue, L. Chen, B. Zhou, M. Shan, J. Niu, B. Li, X. Qian, Chem. Eng. J. 240 (2014) 187–194.
[23] A. Holloway, G. Wildgoose, R. Compton, L. Shao, M. Green, J. Solid State Electrochem. 12 (2008) 1337–1348.
[24] I.Y. Jang, H. Ogata, K.C. Park, S.H. Lee, J.S. Park, Y.C. Jung, Y.J. Kim, Y.A. Kim, M. Endo, J. Phys. Chem. Lett. 1 (2010) 2099–2103.
[25] K.S.W. Sing, D.H. Everett, R.A.W. Haul, L. Moscou, R.A. Pierotti, J. Rouquerol, T. Siemieniewska, Pure Appl. Chem. 57 (1985) 603–619.
[26] O. Barbieri, M. Hahn, A. Herzog, R. Kötz, Carbon 43 (2005) 1303–1310.
[27] B. Xu, S. Yue, Z. Sui, X. Zhang, S. Hou, G. Cao, Y. Yang, Energy Environ. Sci. 4 (2011) 2826–2830.
[28] J. Chmiola, G. Yushin, Y. Gogotsi, C. Portet, P. Simon, P.L. Taberna, Science 313 (2006) 1760–1763.
[29] B.E. Conway, Electrochemical Supercapacitors, Kluwer Academic/ Plenum Publishers, New York, 1999.
[30] A. Krause, A. Balducci, Electrochem. Commun. 13 (2011) 814–817.
[31] D. Wang, F. Li, m: Liu, G. Lu, H. Cheng, Angew. Chem. 47 (2008) 373–376.
[32] C. Vix-Guterl, E. Frackowiak, K. Jurewicz, M. Friebe, J. Parmentier, F. Beguin, Carbon 43 (2005) 1293–1302.
[33] Y. Gogotsi, P. Simon, Science 334 (2011) 917–918.
[34] A. Burke, Electrochim. Acta 53 (2007) 1083–1091.